Metabolic dissimilarity determines the establishment of cross-feeding interactions in bacteria

Samir Giri[1,2,*], Leonardo Oña[2], Silvio Waschina[3,4], Shraddha Shitut[1,2,#], Ghada Yousif[1,2,5], Christoph Kaleta[4], and Christian Kost[1,2,*]

[1] Experimental Ecology and Evolution Research Group, Department of Bioorganic Chemistry, Max Planck Institute for Chemical Ecology, 07745 Jena, Germany
[2] Department of Ecology, School of Biology/Chemistry, University of Osnabrück, 49076 Osnabrück, Germany
[3] Institute for Human Nutrition and Food Science, Nutriinformatics, Christian-Albrechts-University Kiel, 24105 Kiel, Germany
[4] Research Group Medical Systems Biology, Institute for Experimental Medicine, Christian-Albrechts-University Kiel, 24105 Kiel, Germany
[5] Department of Botany and Microbiology, Faculty of Science, Beni-Suef University, Beni-Suef, Egypt

[*] Correspondence: christiankost@gmail.com (CKo), samirgiri2809@gmail.com (SG)

[#] Current address: Institute of Biology, University of Leiden, 2333 Leiden, The Netherlands.

Abstract

The exchange of metabolites among different bacterial genotypes is key for determining the structure and function of microbial communities. However, the factors that govern the establishment of these cross-feeding interactions remain poorly understood. While kin selection theory predicts that individuals should direct benefits preferentially to close relatives, the potential benefits resulting from a metabolic exchange may be larger for more distantly related species. Here we distinguish between these two possibilities by performing pairwise cocultivation experiments between auxotrophic recipients and 25 species of potential amino acid donors. Auxotrophic recipients were able to grow in the vast majority of pairs tested (78%), suggesting that metabolic cross-feeding interactions are readily established. Strikingly, both the phylogenetic distance between donor and recipient as well as the dissimilarity of their metabolic networks was positively associated with the growth of auxotrophic recipients. Finally, this result was corroborated in an *in-silico* analysis of a co-growth of species from a gut microbial community. Together, these findings suggest metabolic cross-feeding interactions are more likely to establish between strains that are metabolically more dissimilar. Thus, our work identifies a new rule of microbial community assembly, which can help predict, understand, and manipulate natural and synthetic microbial systems.

Keywords

Bacterial community, community assembly, cross-feeding, metabolic distance, metabolite secretion, niche overlap, phylogenetic relatedness, public good.

Significance

Metabolic cross-feeding is critical for determining the structure and function of natural microbial communities. However, the rules that determine the establishment of these interactions remain poorly understood. Here we systematically analyze the propensity of different bacterial species to engage in unidirectional cross-feeding interactions. Our results reveal that synergistic growth was prevalent in the vast majority of cases analyzed. Moreover, both phylogenetic and metabolic dissimilarity between donors and recipients favored a successful establishment of metabolite exchange interactions. This work identifies a new rule of microbial community assembly that can help predict, understand, and manipulate microbial communities for diverse applications.

Introduction

Microorganisms are ubiquitous on our planet and are key for driving vital ecosystem processes (1-3). They contribute significantly to the flow of elements in global biogeochemical cycles (3, 4) and are also crucial for determining the fitness of plants (5, 6) and animals (7, 8) including humans (9, 10). These vital functions are provided by complex communities that frequently consist of hundreds or even thousands of metabolically diverse strains and species (11, 12). However, the rules that determine the assembly, function, and evolution of these microbial communities remain poorly understood. Yet understanding the underlying governing principles is central to microbial ecology and crucial for purposefully designing microbial consortia for biotechnological (13) or medical applications (14, 15).

In recent years, both empirical and theoretical work increasingly suggests that the exchange of essential metabolites among different bacterial genotypes is a key process that can significantly affect growth (16, 17), composition (18), and the structure of microbial communities (19). In those cases, one bacterial genotype releases a molecule into the extracellular environment, which can be used by other cells in the local vicinity. The released substances frequently include building block metabolites such as amino acids (20, 21), vitamins (22, 23), or nucleotides (24) as well as degradation products of complex polymers (19, 25). Even though these compounds represent valuable nutritional resources, they are released as unavoidable byproducts of bacterial physiology (26, 27) and metabolism (28) or due to leakage through the bacterial membrane (29, 30). Consequently, the released compounds create a pool of resources that can benefit both conspecifics and members of other species in the local neighborhood (31-34). The beneficiaries include genotypes that opportunistically take advantage of these metabolites as well as strains, whose survival essentially depends on an external supply with the corresponding metabolite. These so-called *auxotrophic*

genotypes carry a mutation in a biosynthetic or regulatory gene, which renders the resulting mutant unable to autonomously produce a certain metabolite such as an amino acid, a vitamin, or a nucleotide. By utilizing metabolites that are produced by another cell, a unidirectional cross-feeding interaction is generated. Auxotrophic mutants that use compounds released by others frequently gain a significant fitness advantage over prototrophic cells that produce the required metabolites by themselves (35). Due to the tremendous benefits that can result from this process, cross-feeding interactions are prevalent in all kinds of microbial ecosystems, including soil (36), fermented food (21), aquatic environments (37, 38), as well as host-associated microbiota (7, 39). Despite the ubiquity of unidirectional cross-feeding interactions in nature, the rules that govern their establishment remain poorly understood (40-43). In particular, it is unclear how the relationship between the metabolite donor and the auxotrophic recipient affects the likelihood that a cross-feeding interaction is successfully established. Two possibilities are conceivable.

First, kin selection theory predicts that organisms should preferentially direct benefits to close relatives rather than to more distantly related individuals (44). In this way, individuals indirectly favor the spread of their own genes. Even if the interaction at this stage is merely created by chance and has not evolved for this purpose, certain mechanisms might be in place that could maximize the chance that cells preferentially interact with conspecifics. Such mechanisms could be based, for example, on recognition alleles, as they play a role in other social interactions such as quorum sensing (45), biofilm formation (46), and swarming (47). Moreover, the exchange of metabolites could be mediated by contact-dependent interactions such as the formation of intercellular nanotubes (48, 49), which might require a close phylogenetic relatedness between donor and recipient for an efficient transport to operate. In the following, we refer to this possibility as the *similarity hypothesis.*

Second, unidirectional cross-feeding interactions might favor more distantly related donor-recipient pairs over interactions among close relatives. Two closely related bacterial cells are more likely to share ecological preferences such as habitat or resources utilized than two phylogenetically different bacterial taxa (41). Moreover, two genealogically related cells have greater similarities in their metabolic network than two distantly related cells (33, 50, 51). As a consequence, the biosynthetic cost to produce a given metabolite, and thus its nutritional value, is more likely to be different in heterospecific pairs than among members of the same species (52, 53). If these differences translate into enhanced growth of the auxotrophic recipient, a positive correlation between the growth of the auxotroph and the phylogenetic and/ or metabolic distance to the donor cell would be observed. In the following, we refer to this alternative possibility as the *dissimilarity hypothesis.*

Here we aim at distinguishing between these two hypotheses to better understand the rules that govern the establishment of this ecologically important interaction. To achieve this goal, we used unidirectional cross-feeding interactions as a model. Synthetically assembling pairs consisting of an auxotrophic recipient and a prototrophic amino acid donor of the same or a different species ensured that both interaction

partners do not share a common evolutionary history. In this way, all results will represent the situation of a naïve encounter between both interaction partners and only mirror effects resulting from the phylogenetic relatedness and metabolic dissimilarity between partners. Using this ecological approach, we systematically determined whether and how the phylogenetic or metabolic distance between auxotrophic recipients and prototrophic amino acid donors affects cross-feeding in pairwise bacterial consortia.

Our results show that in the vast majority of cases, unidirectional cross-feeding interactions successfully established between a prototrophic donor and an auxotrophic recipient. Strikingly, recipients' growth was positively associated with both, the phylogenetic and metabolic distance between donor and recipient. This pattern could partly be explained by the difference in the amino acid profiles produced by donors. Finally, an *in-silico* analysis of co-growth of species from a gut microbial community revealed that recipient genotypes benefitted more when interacting with metabolically dissimilar partners, thus corroborating the empirical results. Our work identifies the metabolic dissimilarity between donor and recipient genotypes as a key parameter for the establishment of unidirectional cross-feeding interactions.

Results

Auxotrophic recipients commonly benefit from the presence of prototrophic donor cells

To determine the probability, with which unidirectional cross-feeding interactions emerge between an auxotrophic recipient and a prototrophic donor genotype, a series of pairwise coculture experiments were performed (Fig. 1A). For this, 25 strains that belonged to 21 different bacterial species were used as potential amino acid donors (Figs. 1B and S1A). Donor strains were selected to cover both the existing diversity of bacterial taxa and the phylogenetic neighborhood of the focal auxotrophs as good as possible. These potential amino acid donors were individually cocultured together with one auxotrophic recipient of *Escherichia coli* or *Acinetobacter baylyi*, which were both auxotrophic for either histidine (Δ*hisD*) or tryptophan (Δ*trpB*) (Fig. S1B).

To test if the selected donor strains can support the growth of auxotrophic recipients, the abovementioned strains were systematically cocultured in all possible pairwise combinations (initial ratio: 1:1). Subsequently, the net growth of the recipient strains in coculture was quantified over 24 h, and compared to the growth, the same strain achieved in monoculture over the same period in the absence of amino acid. In this experiment, the donor's presence affected the recipient's growth either positively, negatively, or in a neutral way. Only 2% of the tested cases showed a growth reduction, and in 20% of the interactions, auxotrophs did not respond at all to the presence of a donor cell (Fig. 1C). In contrast, in the vast majority of cocultures tested (i.e., 78%), auxotrophic cells grew significantly better in the presence of donor cells than monocultures of auxotrophs, suggesting that unidirectional cross-feeding interactions can readily establish (Fig. 1C).

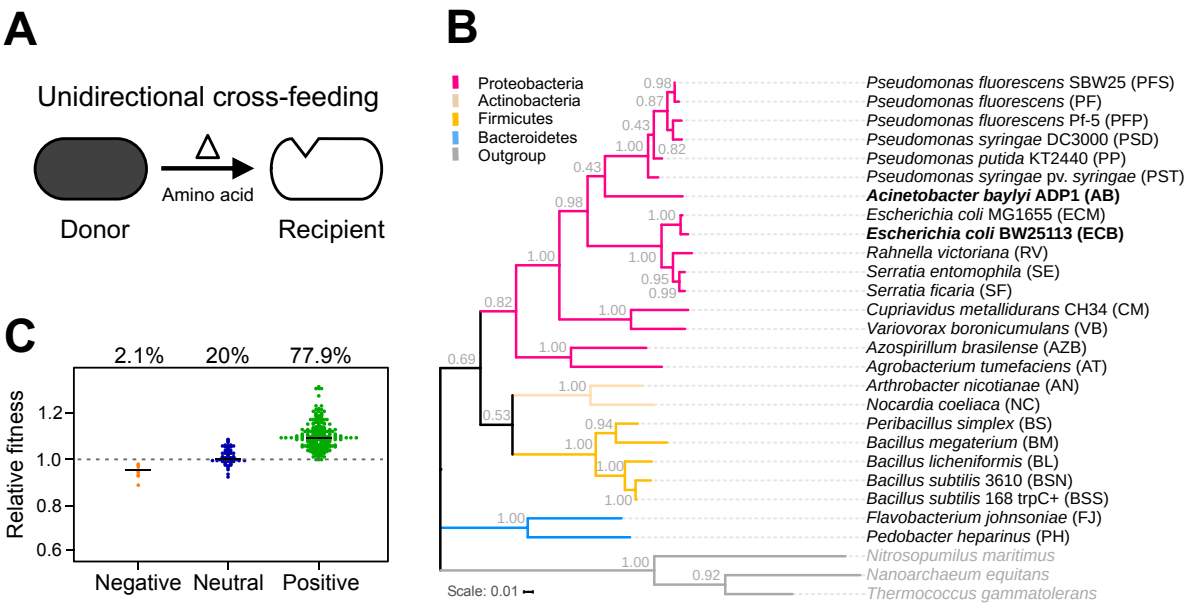

Fig. 1. Unidirectional cross-feeding between prototrophic donor cells and amino acid auxotrophic recipients is common. (A) Overview over the experimental system used. Metabolically autonomous donor genotypes (dark cell) were cocultivated together with an auxotrophic recipient that was unable to produce either histidine or tryptophan (white cell). Growth of auxotrophs signifies the successful establishment of a unidirectional cross-feeding interaction, in which the focal amino acid (△) is exchanged between both cells. **(B)** Phylogenetic tree of bacterial species (donors and recipients) used in this study. Different colors indicate different phyla. The tree was constructed based on the 16S rRNA gene. Recipient strains used in this study are highlighted in bold. Branch node numbers represent bootstrap support values. **(C)** Growth of auxotrophic recipients in pairwise coculture with different donor genotypes. *Escherichia coli* and *Acinetobacter* baylyi, each either auxotrophic for histidine (Δ*hisD)* or tryptophan *(*Δ*trpB),* were used as amino acid recipients. The relative fitness of receivers when grown in coculture with one of X donors is plotted relative to their growth in monoculture in the absence of the focal amino acid (dashed line). CFU was calculated 24 h post-inoculation. Interactions in cocultures were classified as negative (n = 8), neutral (n = 76), and positive (n = 296), based on the statistical difference between the growth of auxotrophs in monoculture and coculture (FDR-corrected paired t-test: $P \leq 0.05$, n = 4).

Recipient growth depends on amino acid production of donor genotypes

The main factor causing the growth of auxotrophs in the coculture experiments was likely the amount and identity of metabolites that donor cells released into the extracellular environment (i.e., the exo-metabolome) (26). To test if amino acid production of donors could explain the observed recipient growth, the supernatant of monocultures of all 25 donor strains was collected during exponential growth. Subjecting the cell-free supernatant of these cultures to LC/MS/MS analysis revealed that all tested genotypes secreted amino acids in varying amounts (Figs. 2A and S2).

A

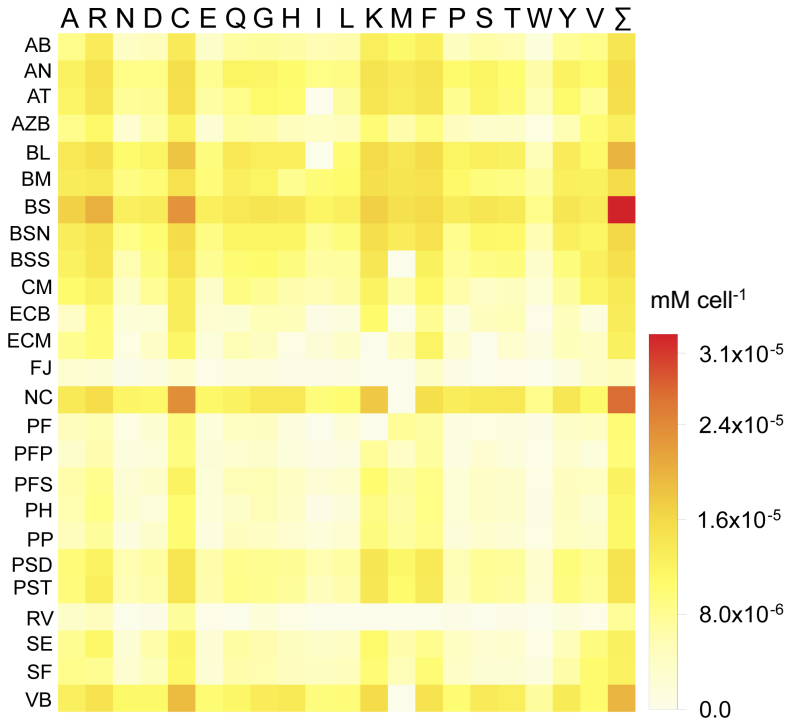

B

Supernatant experiment

Total amino acids			
Recipient	n	ρ	P-value
AB-his	89	0.29	**4.3×10^{-3}**
AB-trp	90	0.17	0.12
ECB-his	92	0.35	**8.3×10^{-4}**
ECB-trp	93	0.33	**1.2×10^{-3}**
Focal amino acid			
AB-his	89	0.23	**0.029**
AB-trp	90	0.09	0.37
ECB-his	92	0.47	**0.2×10^{-5}**
ECB-trp	93	0.43	**0.13×10^{-4}**

Fig. 2. Total amino acids production of different donors can predict unidirectional cross-feeding. (A) Heatmap of amino acids released by different donor strains. Amount of amino acid (mM per cell) produced by 25 donor strains (for abbreviations see Fig. 1B) is shown (Y-axis). Cell-free supernatants of exponentially growing cultures were analyzed via LC/MS/MS. Colors indicate different amino acid concentrations (legend). Σ = total amino acid produced by the donor. **(B)** Overview over the statistical relationships between the total amount of amino acids (upper part) or the focal amino acid (lower part) in supernatants of donor cultures and the growth of the corresponding auxotrophic recipients. Results of spearman rank correlations (ρ) are shown.

In this experiment, donors are not expected to specifically produce the amino acid that the cocultured auxotroph requires for growth. Moreover, bacteria usually use generic

transporters that transport similar types of amino acids across the membrane (54-56). Thus, auxotrophic recipients may benefit not only from the one amino acid they require for growth, but also from utilizing the other amino acids that are produced by the donor. To quantitatively determine whether the released amino acids could explain the growth of recipient cells, the conditioned cell-free supernatant was supplied to monocultures of auxotrophic cells and the resulting growth over 24 h was quantified. In addition, the chemical composition of the supernatants used was determined via LC/MS/MS. This experiment revealed that donor supernatants enhanced the growth of auxotrophic recipients. Interestingly, recipient growth correlated positively with the total amount of amino acids that were present in the supernatant (Table 2B). In addition, growth of auxotrophic recipients was positively associated with the concentration of the amino acid auxotrophs required for growth as well as with the total amount of amino acids produced by donor cells (Table 2B). Together, these results show that auxotrophic recipients not only use the amino acids they cannot produce on their own, but also take advantage of the other amino acids that are produced by donor cells.

Recipient growth correlates positively with amino acid profile dissimilarity

To distinguish between the two main hypotheses, we asked whether the difference in the amino acid profile produced by a closely and distantly related donor strain could explain the growth auxotrophs achieved in the coculture experiment. To test this, we calculated the Euclidean distance between the amino acid profiles of all 25 donor strains. Assessing the statistical relationship between the normalized growth of auxotrophs in coculture with the Euclidean distance in the amino acid profiles of closely and distantly related donor genotypes revealed a significant positive relationship between both parameters in all cases (Fig. 3A and Table 1). In other words, auxotrophs grew better in coculture with a donor, which contained an amino acid mixture that was different from the one a conspecific cell would have produced. Thus, these results provide evidence that supports the dissimilarity hypothesis.

Growth of recipients scales positively with the phylogenetic and metabolic distance to donor cells

Next, we asked whether two phylogenetically close genotypes are more likely to engage in a unidirectional cross-feeding interaction than two more distantly related genotypes. To test this, we re-analyzed the results of the coculture experiment by focusing on the phylogenetic relatedness between donor and recipient genotypes. In this context, only those cocultures were considered, in which auxotrophs showed detectable growth. These analyses revealed a positive association between the growth of recipients and the phylogenetic distance to donor cells (Fig. 3B and Table 1).

However, given that previous analyses suggested that differences in the amino acid profiles could predict auxotrophic recipients' growth (Fig. 3A and Table 1), we hypothesized that the phylogenetic distance might only be a proxy for the difference in the strains' metabolic networks. To verify this hypothesis, we compared genome-scale metabolic networks of all donor and recipient genotypes. Using this data, a metabolic similarity matrix between donor and recipient strains was calculated by identifying

commonalities and differences in both partners' biosynthetic pathways. Correlating the resulting data with the growth of auxotrophic recipients in coculture revealed again a positive association between the metabolic distance and recipient growth (Fig. 3C and Table 1). Together, these results provide additional support for the interpretation that cross-feeding interactions are more likely to establish between two more dissimilar genotypes.

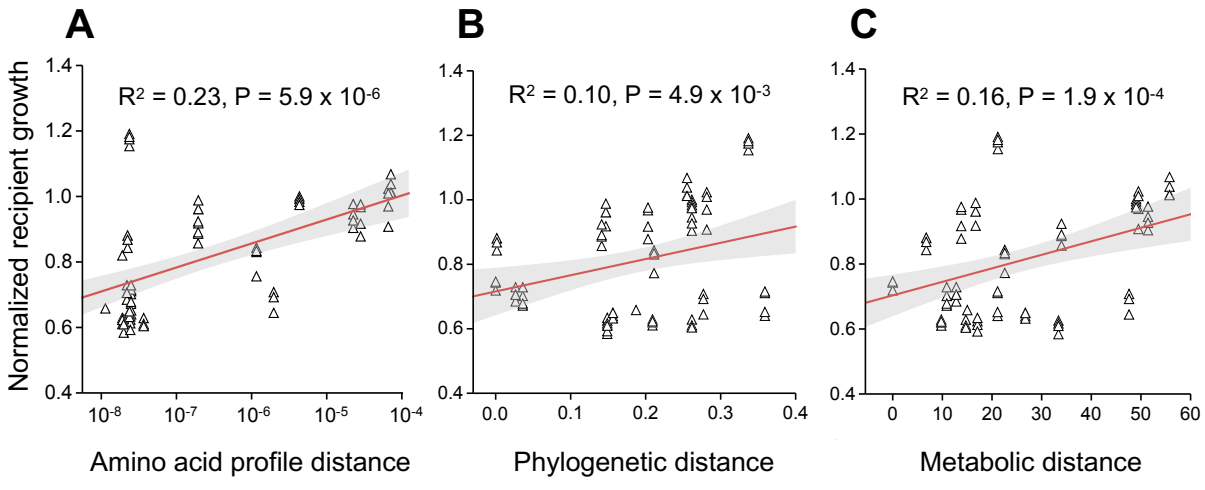

Fig. 3. Cross-feeding increases with an increasing dissimilarity to donor cells. Shown is the net growth of the *E. coli* recipient auxotrophic for histidine (Δ*hisD*, △) as a function of **(A)** the amino acid profile distance, **(B)** the phylogenetic distance, and **(C)** the genome-based metabolic distance between donor and recipient. Red lines are fitted linear regressions and grey area indicates the 95% confidence interval. Sample size is 80 in all cases. Growth of recipient is displayed as a logarithm of the difference in number of CFUs between 0 h and 24 h and was normalized per number of donor cells.

Table 1. Amino acid profile distance (AAD), phylogenetic distance (PD), and metabolic distance (MD), is positively associated with recipient growth. Results of statistical regressions are shown.

		AAD		PD		MD	
Recipient	n	R^2	P-value	R^2	P-value	R^2	P-value
AB-his	87	0.16	**8.0×10^{-5}**	0.45	**1.61×10^{-12}**	0.26	**3.82×10^{-7}**
AB-trp	100	0.07	**5.5×10^{-3}**	0.11	**7.92×10^{-4}**	0.19	**5.59×10^{-6}**
ECB-his	80	0.23	**5.9×10^{-6}**	0.10	**4.95×10^{-3}**	0.16	**1.96×10^{-4}**
ECB-trp	91	0.26	**2.1×10^{-7}**	0.12	**6.40×10^{-4}**	0.17	**3.80×10^{-5}**

All three distance measures alone can explain recipient growth

Having observed a significant positive correlation of recipient growth with each of the three-distance metrics analyzed (i.e., amino acid profile distance (AAD), phylogenetic distance (PD), and metabolic distance (MD), Table 1), we asked whether these factors alone were sufficient to predict the growth of auxotrophic recipients. This question was addressed by replotting the data of the performed coculture experiments in three-dimensional graphs that display the growth of a given auxotroph depending

on two of the three measures quantified. Fitting a 2D plane into the resulting graphs indicated that increasing each of the three measures also increased recipients' growth (Fig. 4 and S3). Thus, these graphs suggested that the three explanatory variables are likely correlating with each other. To subject this conjecture to a formal statistical test, we repeated the regression analyses to examine whether MD or AAD were significantly associated with the growth of auxotrophs in coculture, when the first predictor variable PD was already included (Table S1). In all cases, growth of *E. coli* recipients remained positively associated with metabolic distance as well as the distance of the amino acid production profile (Table S1). However, this pattern no longer holds for *A. baylyi* auxotrophs (Δ*hisD* and Δ*trpB*) (Table S1).

Furthermore, we hypothesize that the amount of amino acid produced by the donors should affect recipient growth. Genotypically related donors are more likely to produce the same spectrum of amino acids as compared to distantly related individuals. In order to consider this fact, we performed additional analyses that controlled for the role of total amino acid production or focal amino acid production (his or trp). In almost all cases, growth of recipients remained significantly positively associated with the three distance measures (Table S2 and S3). Together, the set of analyses performed demonstrates that the three different measures analyzed (i.e., AAD, PD, and MD, and) can individually (in the case of *E. coli*) or in combination (both species) explain the cross-feeding between prototrophic donors and auxotrophic recipients, thus, corroborating the dissimilarity hypothesis.

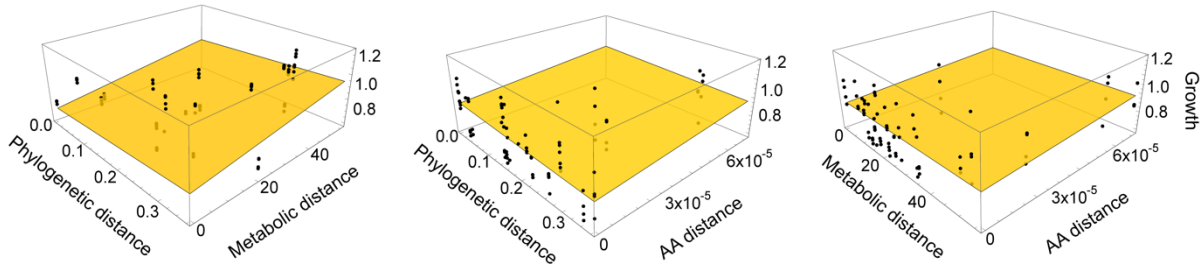

Fig. 4. Multiple distance measures interactively explain recipient growth. The plane depicts the linear regression between the growth of the histidine auxotrophic *E. coli* recipient (Δ*hisD*) and the phylogenetic distance, the metabolic distance, and the amino acid profile distance between donor and recipient. Data points above the plane are shown in black. See also Fig. S3 for other comparisons.

In-silico models predict that metabolic dissimilarity between species enhances cross-feeding

To verify whether the patterns we observed in laboratory-based coculture experiments also apply to natural microbial communities, we used *in-silico* modeling to simulate the co-growth of different bacterial species that co-occur in the human gastrointestinal tract. Specifically, we considered all of 334,153 pairwise combinations of 818 bacteria commonly found in this environment. The *in-silico* simulations indicated that the relationship between metabolic distance and metabolic exchange (i.e., total metabolic fluxes between species) follows a saturation curve (Fig. 5). In fact, fitting a logistic function resulted in a higher goodness of fit ($P < 0.001$, $R^2 = 0.04$) than fitting

a linear function (R^2 = 0.023). This finding suggests that also bacteria residing within the human gut are more likely to engage in cross-feeding interactions with metabolically more dissimilar species. Taken together, the set of computational analyses performed here is in line with the experimental data shown above: both datasets reveal that metabolic cross-feeding interactions are more likely to establish between two metabolically more dissimilar partners.

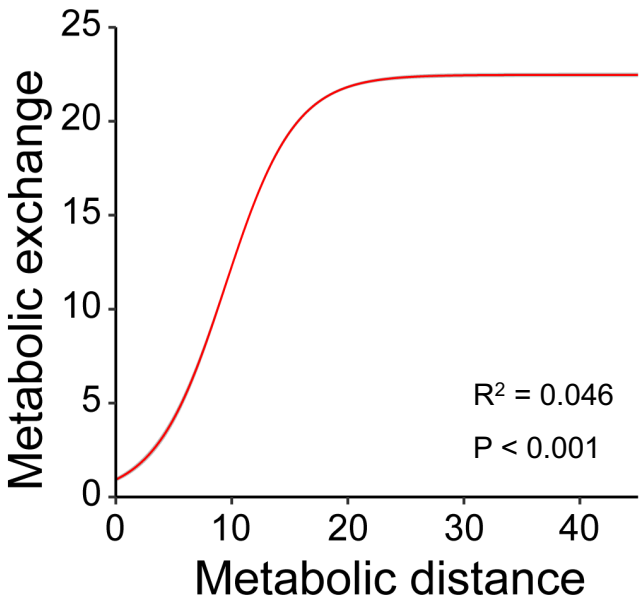

Fig. 5. Metabolic exchange increases with an increasing metabolic distance between interaction partners in gut microbial communities. Shown is the result of an *in-silico* flux-balance-analysis of paired models analyzing 334,153 combinations of 818 bacterial species residing in the human gut. Results of a logistic model (red line) and the 95% confidence interval (grey area) are displayed.

Discussion

Metabolic cross-feeding interactions among different microbial species are ubiquitous and play key roles in determining the structure and function of microbial communities (16, 57, 58). However, the rules that govern their establishment remain poorly understood. Here we identify the metabolic dissimilarity between donor and recipient genotype as a major determinant for the establishment of obligate, unidirectional cross-feeding interactions between two bacterial strains. In systematic coculture experiments between a prototrophic amino acid donor and an auxotrophic amino acid recipient, we show that growth of auxotrophic recipients in coculture was positively associated with (i) the compositional difference in the amino acid mixtures various donor produced (Fig. 3A), (ii) their phylogenetic distance (Fig. 3B), as well as (iii) the difference in their metabolic networks (i.e. their metabolic distance) (Fig. 3C). Furthermore, *in-silico* simulations of the co-growth of species from a gut microbial community corroborated that the propensity of cross-feeding interactions to establish increased when both interacting partners were metabolically more dissimilar (Fig 5).

In our study, we manipulated the relatedness between donor and recipient genotypes. A high phylogenetic relatedness between two genotypes (donor and recipient) in coculture means that they can perform similar metabolic reactions and are more likely to be characterized by overlapping growth requirements (33, 43). As a consequence, both the nutritional value of a given molecule and the biosynthetic cost to produce it is alike (52, 53, 59). In contrast, two phylogenetically distant strains likely differ in their metabolic capabilities and requirements. Thus, two more closely related strains are likely to compete for environmentally available nutrients and provide an increased potential for a difference in the cost-to-benefit-ratio than two distant relatives (43, 60). This statistical relationship can explain why in our coculture experiments, both the phylogenetic and metabolic distance was positively associated with the growth of cocultured auxotrophs. Thus, our results support the dissimilarity hypothesis to explain the establishment of unidirectional cross-feeding interactions. Our findings are in line with previous studies that analyzed the effect of the phylogenetic relatedness and metabolic dissimilarity on antagonistic interactions between two different genotypes. The authors of these studies found that bacteria mainly inhibit the growth of metabolically more similar and related species (41, 61). Even though the focal biological process differs drastically between our (metabolic cross-feeding) and these other studies (antagonistic interactions), the main finding is conceptually equivalent: genotypes are more likely to compete against close relatives, yet support the growth of more dissimilar strains – either by enhancing their growth (Fig. 3) or inhibiting them less (41, 61).

In our experiments, we took advantage of synthetically assembled pairwise interactions between different bacterial genotypes to assess how the similarity between interacting partners affects the cross-feeding of metabolites. Even though this approach is limited by the number of pairwise comparisons that can be analyzed in one experiment, the obtained results provide a very clear answer to the focal question. First, the selected donor strains covered a broad range of taxonomic diversity in bacteria (Fig. 1B). Thus, the spectrum of ecological interactions analyzed here likely reflects the range of interactions a given bacterial genotype would typically experience in a natural microbial community. Second, by deliberately choosing strains that lack a previous coevolutionary history, any result observed can be clearly attributed to the focal, experimentally-controlled parameter (e.g., phylogenetic or metabolic distance). In this way, confounding effects like an evolved preference for a certain genotype can be ruled out. Finally, we analyzed bacterial consortia in a well-mixed, spatially unstructured environment, in which the exchanged metabolites are transferred between cells via diffusion through the extracellular environment. Such a set-up minimizes factors that would be amplified in a spatially structured environment, such as a local competition for nutrients or the release of metabolic waste products that inhibit the growth of other cells in the local vicinity. Thus, the experimental approach chosen circumvents the challenges of manipulating and detecting metabolite exchange in natural environments and instead capitalizes on analyzing experimentally arranged and carefully controlled coculture experiments.

The guiding principle discovered in this study is most likely relevant for ecological interactions outside the realm of microbial communities. Mutualistic interactions, in which two partners reciprocally exchange essential metabolites or services, usually involve two or more completely unrelated species (60, 62-64). In contrast, cooperative interactions among closely related individuals usually rely on the uni- or bidirectional exchange of the same commodity or service (60). Thus, the fact that two more dissimilar individuals have an increased potential to engage in a synergistic interaction than two more similar individuals may be a universal rule that guides the establishment of mutualistic interactions in general (43).

Our results highlight the utility of using synthetic, laboratory-based model systems to understand fundamental principles of microbial ecology. In this study, we demonstrated that the establishment of interactions in complex natural communities is likely determined by simple rules of assembly. These insights not only enrich our understanding of complex microbial communities, but also help us to engineer them for biotechnological or medical applications.

Material and methods

Bacterial strains and their construction

Twenty-five bacterial wild type strains were used as potential amino acid donors (Supplemental Table S4). *Escherichia coli* BW25113 and *Acinetobacter baylyi* ADP1 were used as parental strains, from which mutants that are auxotrophic for histidine (Δ*hisD*) or tryptophan (Δ*trpB*) were generated. The gene to be deleted in order to create the corresponding auxotrophy was identified using the KEGG (65) and the EcoCyc (66) database. For *E. coli*, deletion alleles were transferred from existing single gene deletion mutants (i.e. the Keio collection, (67)) into *E. coli* BW25113 using phage P1-mediated transduction (68). In-frame knockout mutants were achieved by the replacement of target genes with a kanamycin resistance cassette. In the case of *A. baylyi*, deletion mutants were constructed as described previously (48). Briefly, linear constructs of the kanamycin resistance cassette with 5'-overhangs homologous to the insertion site were amplified by PCR, where pKD4 was used as a template (see Supplemental Table S5 for primer details). Upstream and downstream regions homologous to *hisD* and *trpB* were amplified using primers with a 5'-extension that was complementary to the primers used to amplify the kanamycin resistance cassette. The three amplified products (upstream, downstream, and kanamycin) were combined by PCR, resulting in overhanging flanks with a kanamycin cassette. This PCR product was introduced into the *A. baylyi* WT strain. For this, the natural competence of *A. baylyi* was harnessed. Transformation was done by diluting 20 µl of a 16 h-grown culture in 1 ml lysogeny broth (LB). This diluted culture was mixed with 50 µl of the above PCR mix and further incubated at 30 ˚C with shaking at 200 rpm for 3 h. Lastly, 1 ml volume was pelleted, washed once with LB broth, plated on LB agar plates containing kanamycin (50 µg ml^{-1}), and incubated at 30 ˚C for colonies to grow.

Conditional lethality of constructed auxotrophic mutations in MMAB medium was verified by inoculating 10^5 colony-forming units (CFU) ml^{-1} of these strains into 1 ml MMAB medium with or without the focal amino acid (100 μM). After 24 h, their optical density (OD) was determined spectrophotometrically at 600 nm using FilterMax F5 multi-mode microplate reader (Molecular Devices) and the mutation was considered conditionally essential when growth did not exceed the OD_{600nm} of uninoculated minimal medium (67, 69).

Culture conditions and general procedures

A modified minimal media for *Azospirillum brasilense* (MMAB, (70)) was used for all experiments containing K_2HPO_4 (3 g L^{-1}), NaH_2PO_4 (1 g L^{-1}), KCl (0.15 g L^{-1}), NH_4Cl (1 g L^{-1}), $MgSO_4 \cdot 7H_2O$ (0.3 g L^{-1}), $CaCl_2 \cdot 2H_2O$ (0.01 g L^{-1}), $FeSO_4 \cdot 7H_2O$ (0.0025 g L^{-1}), $Na_2MoO_4 \cdot 2H_2O$ (0.05 g L^{-1}), and 5 g L^{-1} D-glucose as a carbon source. 10 ml of trace salt solution was added per liter of MMAB media from the 1L stock. Trace salt stock solution consisted of filter sterilized 84 mg L^{-1} of $ZnSO_4 . 7H_2O$, 765 µl from 0.1 M stock of $CuCl_2 . 2H_2O$, 8.1 µl from 1 M stock of $MnCl_2$, 210 µl from 0.2 M stock of $CoCl_2 . 6H_2O$, 1.6 ml from 0.1 M stock of H_3BO_3, 1 ml from 15 gL^{-1} stock of $NiCl_2$.

All strains were precultured in replicates by picking single colonies from LB agar plates, transferring them into 1 ml of liquid MMAB in 96-deep well plate (Eppendorf, Germany), and incubating these cultures for 20 h. In all experiments, auxotrophs were precultured at 30 ˚C in MMAB, which was supplemented with 100 µM of the required amino acid. The next day, precultures were diluted to an optical density of 0.1 at 600 nm as determined by FilterMax F5 multi-mode microplate readers (Molecular Devices).

Coculture experiment

Approximately 50 µl of preculture were inoculated into 1 ml MMAB, leading to a starting density 0.005 OD. In case of cocultures, donor and recipient were mixed in a 1:1 ratio by co-inoculating 25 µl of each diluted preculture without amino acid supplementation. Monocultures of both donors and recipient (with and without the focal amino acid) were inoculated using 50 µl of preculture. Cultures were incubated at a temperature of 30 ˚C and shaken at 220 rpm. Cell numbers were determined at 0 h and 24 h by serial dilution and plating. Donor strains were plated on MMAB agar plates, whereas recipients (auxotrophs) were differentiated on LB agar containing kanamycin (50 μg ml^{-1}) to select for recipient strains. For key resources, see (Supplemental Table S6).

Relative fitness measurement

To quantify the effect of amino acid cross-feeding on the fitness of the recipient, the number of colony-forming units (CFU) per ml was calculated for monoculture and coculture conditions at 0 h and 24 h. Each donor was individually paired with one of the recipients as well as grown in monoculture. Every combination was replicated four times. The relative fitness of each recipient was determined by dividing the growth of each genotype achieved in coculture by the value of its respective monoculture. Since different donor genotypes show inherent differences in growth, the growth of recipients in coculture was normalized to reduce to minimize potential effects of this variation.

For this, growth of recipients in monoculture was first subtracted from its growth in coculture and then divided by the growth the respective donor genotype achieved in coculture.

Amino acid supernatant experiment

To determine whether cross-feeding was mediated via compounds that have been released into the extracellular environment, the cell-free supernatants of donor genotypes were harvested and provided to receiver strains. To collect the supernatant, donors were grown in 2.5 ml MMAB in 48-deep well plates (Axygen, USA) and cultivated at 30 ˚C under shaking conditions (220 rpm). Supernatants were isolated in the mid-exponential growth phase and centrifuged for 10 min at 4,000 rpm. Then, supernatants were filter-sterilized (0.22 µm membrane filter, Pall Acroprep, USA) and stored at -20 ˚C. Meanwhile, receivers were grown in 1 ml MMAB in 96-well plates for 24 h. After adjusting the receiver OD_{600nm} to 0.1, 5 µl of the receiver culture was added to the replenished donor supernatant (total culturing volume: 200 µl, i.e. 160 µl donor supernatant + 40 µl MMAB) in 384-well plates (Greiner bio-one, Austria) (total: 50 µl culture). Four replicates of each comparison were grown for 24 h at 30 ˚C in a FilterMax F5 multi-mode microplate reader (Molecular Devices). MMAB without supernatant and monocultures of receiver strains were used as control. Growth was determined by measuring the optical density at 600 nm every 30 minutes, with 12 minutes of orbital shaking between measurements. OD_{600nm} was measured and analyzed to calculate the maximum optical density (OD_{max}) achieved by the receiver strain usingthe Softmax Pro 6 software (Table S7). For each donor supernatant-receiver pair, OD_{max} achieved by receivers with supernatant was subtracted from the values achieved by cultures grown without supernatant and normalized with the OD_{600nm}, the respective donor strain had achieved at the time of supernatant extraction.

Amino acid quantification by LC/MS/MS

All 20 proteinogenic amino acids in the culture supernatant were analyzed. 100 µl of extracted supernatant was derivatized using the dansyl chloride method (71, 72). Norleucine was added as an internal standard to the sample and a calibration curve was generated by analyzing all 20 amino acids at different concentrations. All samples were directly analyzed via LC/MS/MS. Chromatography was performed on a Shimadzu HPLC system. Separation was achieved on an Accucore RP-MS 150 x 2.1, 2,6 µm column (Thermo Scientific, Germany). Formic acid 0.1% in 100% water and 80% acetonitrile were employed as mobile phases A and B, respectively. The mobile phase flow rate was 0.4 ml min^{-1} and the injection volume was 1 µl. Liquid chromatography was coupled to a triple-quadrupole mass spectrometer (ABSciex Q-trap 5500). Other parameters were: curtain gas: 40 psi, collision gas: high, ion spray voltage (IS): 2.5 keV, temperature: 550 ˚C, ion source gas: 1: 60 psi, ion source gas 2: 70 psi. Multiple reaction monitoring was used to determine the identity of the focal analyte. Analyst and Multiquant software (AB Sciex) were used to extract and analyze the data.

Amino acid profile-based distance calculation using supernatant data

The similarity between closely related and distantly related donor amino acid profiles was measured by calculating the Euclidean distance. If the amino acid production of a closely related donor is given by $CR = (cr_1, cr_2, \cdots, cr_{20})$, and the amino acid production of the distant related donor is given by $DR = (dr_1, dr_2, \cdots, dr_{20})$, the Euclidean distance between recipient and donor is:

$$ED(CR, DR) = \sqrt{(cr_1 - dr_1)^2 + (cr_2 - dr_2)^2 + \cdots + (cr_{20} - dr_{20})^2}$$

Index numbers (1-20) refer to individual amino acids.

Phylogenetic tree construction and distance calculation

To cover a broad taxonomic diversity of donor strains, we chose 25 well-characterized species, belonging to four different phyla. The 16S rRNA gene sequences of 20 strains were retrieved from the NCBI GenBank and 5 strains from 16S rRNA sequencing (see supplementary method). The phylogenetic tree of this marker gene was generated using the maximum likelihood method in MEGA X software (73). 16S rRNA gene locus sequences of all strains were converted to amino acid sequences and aligned with MUSCLE. Maximum-likelihood (ML) trees were constructed using the Kimura 2-parameter model, where rates and patterns among mutated sites were kept at uniform rates, yielding the best fit. Bootstrapping was carried out with 1,000 replicates. The phylogenetic tree was edited using the iTOL online tool (Table S7) (74). Pairwise phylogenetic distances between donor and receiver strains were extracted from a phylogenetic distance-based matrix. The resulting values quantify the evolutionary distance that separates the organisms.

Reconstruction of metabolic networks

Genome-scale metabolic networks for all organisms (Table S4) were reconstructed based on their genomic sequences using the GapSeq software (version v0.9, https://github.com/jotech/gapseq) (75). In brief, the reconstruction process is divided in two main steps. First, reactions and pathway predictions, and, second, gap-filling of the network to facilitate *in-silico* biomass production using flux balance analysis. For the reaction and pathway prediction step, all pathways from MetaCyc database (76) that are annotated for the taxonomic range of bacteria, were considered. Of each reaction within pathways, the protein sequences of the corresponding enzymes were retrieved from the SwissProt database (77) and aligned against the organism's genome sequence by the TBLASTN algorithm (78). An enzyme, and thus the corresponding reaction, was considered to be present in the organism's metabolic network, if the alignment's bitscore was ≥ 200 and the query coverage ≥ 75%. Moreover, reactions were considered to be existing, if more than 75% of the remaining reactions within the pathway were predicted to be present by the BLAST-searches or if more than 66% of the key enzymes, which are defined for each pathway by MetaCyc, were predicted to be part of the network by the blast searches. As reaction database for model construction, we used the ModelSEED database for metabolic modeling (79).

The second step (i.e., the gap filling algorithm of gapseq) solves several optimization problems by utilizing a minimum number of reactions from the ModelSEED database and adding them to the network, in order to facilitate growth in a given growth medium. Here, the chemical composition of the M9 medium (which is qualitatively identical to MMAB) with glucose as sole carbon source was assumed.

Calculating the genome-based metabolic distance of organisms

To estimate the pairwise metabolic distance between donor and recipient genotypes, the structure of their metabolic network was compared. For this, a flux balance analysis was performed on each individual metabolic network model. Subsequently, total flux was minimized to predict the flux distribution in M9-glucose medium (80). Pairwise distances of flux distributions between organisms were calculated as the Euclidean distance between the predicted flux vectors. Only reactions with a non-zero flux in at least one of the two organisms were included in the distance approximations.

In-silico *simulation of bacterial co-growth*

To further investigate the relationship between the metabolic distance between organisms and the likelihood for them to enter into a cross-feeding interaction, we extended our analysis to a larger number of bacterial organisms using *in-silico* co-growth simulations. For this, we reconstructed 818 bacterial metabolic network models as described above. The selected 818 organisms are the same as from the AGORA-collection, which represent common members of the human gut microbiota (81). For co-growth simulations, the models were merged in a pairwise manner as described previously (82). The predicted metabolic flux distributions of bacterial co-growth simulations were used to estimate the *metabolic exchange* between organisms. The metabolic exchange between two organisms was calculated as the sum of absolute predicted exchange rates (exchange fluxes) of metabolites. A logistic curve function of the form $y(x) = a / (1 + e^{-b*(x-c)})$ was fitted to the data using R (83).

Statistical data analysis

Normal distribution of data was evaluated by means of the Kolmogorov-Smirnov test and data was considered to be normally distributed when $P > 0.05$. Homogeneity of variance was determined using Levene's test and variances were considered homogenous if $P > 0.05$. Differences in the recipient growth in coculture versus monocultures were assessed with paired sample t-tests. P-values were corrected for multiple testing by applying the false discovery rate (FDR) procedure of Benjamini *et al.* (84, 85). Linear regressions were used to assess the growth support of recipients in cocultures as a function of different variables (i.e. amino acid profile distance, phylogenetic distances, metabolic distance). Spearman's rank correlation was used to assess the relationship between amino acid production and growth of recipient as maximum density when cultured with donor supernatants. The relationship between each proxy tested and recipient growth was depicted as a 2D plane and analyzed by

fitting a linear regression. Regression analyses was also used to disentangle the effect of more than one interacting predictor variable. In these cases, the phylogenetic signal or amino acid produced was controlled for the respective other predictor variable (e.g. metabolic distance or amino acid production profile distance) used to predict growth of recipient (Table S7).

Acknowledgements

We thank the entire Kost lab (past and present) for useful discussion as well as Marita Hermann and Antje Moehlmeyer for technical assistance. We are grateful to Stefan Walter and Saskia Schuback (CellNanOS, MS facility) for help with quantifying the exo-metabolome, Heiko Vogel and Domenica Schnabelrauch (Department of Entomology, MPI-CE) for help in 16s rRNA sequencing, Ákos T. Kovács, (Technical University of Denmark; Denmark) for sharing two *Bacillus subtilis* strains and Michael Hensel, (Department of Microbiology, University of Osnabrück; Germany) for providing *Serratia ficaria* strain. This work was funded by the German Research Foundation (SPP1617, KO 3909/2-1: CK, SG), (SFB 944, P19: CK), (KO 3909/4-1: CK), and the University of Osnabrück (LO, *EvoCell*: CK). CKa and SW acknowledge support by the German Research Foundation within the scope of the Excellence Cluster “Precision medicine in chronic inflammation” (EXC2167, sub-project RTF-VIII) and the Collaborative research center “Metaorganisms” (SFB1182, sub-project A1).

Author contributions

SG and CKo conceived the project. SG, SS, and CKo designed the research. SG performed all experiments. SG and LO analyzed the data. SG, LO, and CKo interpreted the data. SW calculated the genome-scale metabolic distance of tested strains and performed all *in-silico* analyses. SW and CKa carried out the gut microbiome *in-silico* data collection. GY isolated and phenotypically characterized the five environmentally-derived donor strains. SG and CKo wrote the manuscript, all authors revised the manuscript. CKo provided resources and acquired funding.

Competing interests

The authors declare no competing interests.

References

1. N. Fierer, R. B. Jackson, The diversity and biogeography of soil bacterial communities. *Proceedings of the National Academy of Sciences of the United States of America* **103**, 626-631 (2006).
2. C. A. Lozupone, R. Knight, Global patterns in bacterial diversity. *Proceedings of the National Academy of Sciences* **104**, 11436-11440 (2007).
3. P. G. Falkowski, T. Fenchel, E. F. Delong, The microbial engines that drive earth's biogeochemical cycles. *Science* **320**, 1034-1039 (2008).

4. N. Fierer, Embracing the unknown: disentangling the complexities of the soil microbiome. *Nature Reviews Microbiology* **15**, 579-590 (2017).
5. R. Mendes *et al.*, Deciphering the rhizosphere microbiome for disease-suppressive bacteria. *Science* **332**, 1097-1100 (2011).
6. M. Saleem, J. Hu, A. Jousset, More than the sum of its parts: microbiome biodiversity as a driver of plant growth and soil health. *Annual Review of Ecology, Evolution, and Systematics* **50**, 145-168 (2019).
7. C. W. Russell *et al.*, Matching the supply of bacterial nutrients to the nutritional demand of the animal host. *Proceedings of the Royal Society B: Biological Sciences* **281**, 20141163 (2014).
8. W. K. Kwong *et al.*, Dynamic microbiome evolution in social bees. *Science Advances* **3**, e1600513 (2017).
9. A. L. Kau, P. P. Ahern, N. W. Griffin, A. L. Goodman, J. I. Gordon, Human nutrition, the gut microbiome and the immune system. *Nature* **474**, 327-336 (2011).
10. S. V. Lynch, O. Pedersen, The human intestinal microbiome in health and disease. *New England Journal of Medicine* **375**, 2369-2379 (2016).
11. G. E. Leventhal *et al.*, Strain-level diversity drives alternative community types in millimetre-scale granular biofilms. *Nature Microbiology* **3**, 1295-1303 (2018).
12. D. W. Rivett, T. Bell, Abundance determines the functional role of bacterial phylotypes in complex communities. *Nature Microbiology* **3**, 767-772 (2018).
13. S. Giri, S. Shitut, C. Kost, Harnessing ecological and evolutionary principles to guide the design of microbial production consortia. *Current Opinion in Biotechnology* **62**, 228-238 (2020).
14. W. Kong, D. R. Meldgin, J. J. Collins, T. Lu, Designing microbial consortia with defined social interactions. *Nature Chemical Biology* **14**, 821-829 (2018).
15. C. Rezzoagli, E. T. Granato, R. Kümmerli, Harnessing bacterial interactions to manage infections: a review on the opportunistic pathogen *Pseudomonas aeruginosa* as a case example. *Journal of Medical Microbiology* **69**, 147-161 (2020).
16. G. D'Souza *et al.*, Ecology and evolution of metabolic cross-feeding interactions in bacteria. *Natural Product Reports* **35**, 455-488 (2018).
17. K. Zengler, L. S. Zaramela, The social network of microorganisms — how auxotrophies shape complex communities. *Nature Reviews Microbiology* **16**, 383-390 (2018).
18. O. X. Cordero, M. S. Datta, Microbial interactions and community assembly at microscales. *Current Opinion in Microbiology* **31**, 227-234 (2016).
19. T. N. Enke *et al.*, Modular assembly of polysaccharide-degrading marine microbial communities. *Current Biology* **29**, 1528-1535.e1526 (2019).
20. S. Sieuwerts *et al.*, Mixed-culture transcriptome analysis reveals the molecular basis of mixed-culture growth in *Streptococcus thermophilus* and *Lactobacillus bulgaricus*. *Applied and Environmental Microbiology* **76**, 7775-7784 (2010).
21. O. Ponomarova *et al.*, Yeast creates a niche for symbiotic lactic acid bacteria through nitrogen overflow. *Cell Systems* **5**, 345-357.e346 (2017).
22. M. T. Croft, A. D. Lawrence, E. Raux-Deery, M. J. Warren, A. G. Smith, Algae acquire vitamin B12 through a symbiotic relationship with bacteria. *Nature* **438**, 90-93 (2005).
23. O. M. Sokolovskaya, A. N. Shelton, M. E. Taga, Sharing vitamins: Cobamides unveil microbial interactions. *Science* **369**, eaba0165 (2020).
24. A. Loera-Muro *et al.*, Auxotrophic *Actinobacillus pleurpneumoniae* grows in multispecies biofilms without the need for nicotinamide-adenine dinucleotide (NAD) supplementation. *BMC Microbiology* **16**, 128 (2016).

25. S. Rakoff-Nahoum, Michael J. Coyne, Laurie E. Comstock, An ecological network of polysaccharide utilization among human intestinal symbionts. *Current Biology* **24**, 40-49 (2014).
26. N. Paczia *et al.*, Extensive exometabolome analysis reveals extended overflow metabolism in various microorganisms. *Microb. Cell. Fact.* **11**, 122 (2012).
27. A. E. Douglas, The microbial exometabolome: ecological resource and architect of microbial communities. *Philosophical Transactions of the Royal Society B: Biological Sciences* **375**, 20190250 (2020).
28. K. Campbell, L. Herrera-Dominguez, C. Correia-Melo, A. Zelezniak, M. Ralser, Biochemical principles enabling metabolic cooperativity and phenotypic heterogeneity at the single cell level. *Current Opinion in Systems Biology* **8**, 97-108 (2018).
29. B. Schink, Synergistic interactions in the microbial world. *Antonie van Leeuwenhoek* **81**, 257-261 (2002).
30. J. J. Morris, Black Queen evolution: the role of leakiness in structuring microbial communities. *Trends in Genetics* **31**, 475-482 (2015).
31. O. X. Cordero, L.-A. Ventouras, E. F. DeLong, M. F. Polz, Public good dynamics drive evolution of iron acquisition strategies in natural bacterioplankton populations. *Proceedings of the National Academy of Sciences* **109**, 20059-20064 (2012).
32. M. Schuster, D. J. Sexton, S. P. Diggle, E. P. Greenberg, Acyl-homoserine lactone quorum sensing: from evolution to application. *Annual Review of Microbiology* **67**, 43-63 (2013).
33. A. Zelezniak *et al.*, Metabolic dependencies drive species co-occurrence in diverse microbial communities. *Proceedings of the National Academy of Sciences* **112**, 6449-6454 (2015).
34. S. Giri, S. Waschina, C. Kaleta, C. Kost, Defining division of labor in microbial communities. *Journal of Molecular Biology* **23,** 4712-4731 (2019).
35. S. J. Giovannoni, J. Cameron Thrash, B. Temperton, Implications of streamlining theory for microbial ecology. *The ISME Journal* **8**, 1553-1565 (2014).
36. R. Baran *et al.*, Exometabolite niche partitioning among sympatric soil bacteria. *Nature Communications* **6**, 8289 (2015).
37. E. Butaite, M. Baumgartner, S. Wyder, R. Kummerli, Siderophore cheating and cheating resistance shape competition for iron in soil and freshwater *Pseudomonas* communities. *Nat Commun* **8**, 414 (2017).
38. S. L. Garcia *et al.*, Auxotrophy and intrapopulation complementary in the 'interactome' of a cultivated freshwater model community. *Molecular Ecology* **24**, 4449-4459 (2015).
39. S. J. Macdonald, G. G. Lin, C. W. Russell, G. H. Thomas, A. E. Douglas, The central role of the host cell in symbiotic nitrogen metabolism. *Proceedings of the Royal Society B: Biological Sciences* **279**, 2965-2973 (2012).
40. A. Narwani, M. A. Alexandrou, T. H. Oakley, I. T. Carroll, B. J. Cardinale, Experimental evidence that evolutionary relatedness does not affect the ecological mechanisms of coexistence in freshwater green algae. *Ecology Letters* **16**, 1373-1381 (2013).
41. J. Russel, H. L. Roder, J. S. Madsen, M. Burmolle, S. J. Sorensen, Antagonism correlates with metabolic similarity in diverse bacteria. *Proc Natl Acad Sci U S A* **114**, 10684-10688 (2017).
42. C. Xenophontos, M. Taubert, W. S. Harpole, K. Küsel, Phylogenetic and functional diversity have contrasting effects on the ecological functioning of bacterial communities. *bioRxiv* 10.1101/839696, 839696 (2019).
43. D. Machado *et al.*, Polarization of microbial communities between competitive and cooperative metabolism. *bioRxiv* 10.1101/2020.01.28.922583, 2020.2001.2028.922583 (2020).

44. D. Wall, Kin Recognition in Bacteria. *Annu Rev Microbiol* **70**, 143-160 (2016).
45. M. Wang, A. L. Schaefer, A. A. Dandekar, E. P. Greenberg, Quorum sensing and policing of *Pseudomonas aeruginosa* social cheaters. *Proceedings of the National Academy of Sciences* **112**, 2187-2191 (2015).
46. S. Smukalla *et al.*, FLO1 is a variable green beard gene that drives biofilm-like cooperation in budding yeast. *Cell* **135**, 726-737 (2008).
47. P. Stefanic, B. Kraigher, N. A. Lyons, R. Kolter, I. Mandic-Mulec, Kin discrimination between sympatric *Bacillus subtilis* isolates. *Proceedings of the National Academy of Sciences* **112**, 14042-14047 (2015).
48. S. Pande *et al.*, Metabolic cross-feeding via intercellular nanotubes among bacteria. *Nature Communications* **6**, 6238 (2015).
49. S. Shitut, T. Ahsendorf, S. Pande, M. Egbert, C. Kost, Nanotube-mediated cross-feeding couples the metabolism of interacting bacterial cells. *Environ Microbiol* **21**, 1306-1320 (2019).
50. S. Bernhardsson, P. Gerlee, L. Lizana, Structural correlations in bacterial metabolic networks. *BMC Evolutionary Biology* **11**, 20 (2011).
51. E. R. Hester, M. S. M. Jetten, C. U. Welte, S. Lücker, Metabolic overlap in environmentally diverse microbial communities. *Frontiers in Genetics* **10** (2019).
52. S. Waschina, G. D'Souza, C. Kost, C. Kaleta, Metabolic network architecture and carbon source determine metabolite production costs. *The FEBS Journal* **283**, 2149-2163 (2016).
53. H. Akashi, T. Gojobori, Metabolic efficiency and amino acid composition in the proteomes of *Escherichia coli* and *Bacillus subtilis*. *Proceedings of the National Academy of Sciences* **99**, 3695-3700 (2002).
54. N. P. Zakataeva, V. V. Aleshin, I. L. Tokmakova, P. V. Troshin, V. A. Livshits, The novel transmembrane *Escherichia coli* proteins involved in the amino acid efflux. *FEBS Letters* **452**, 228-232 (1999).
55. V. Doroshenko *et al.*, YddG from *Escherichia coli* promotes export of aromatic amino acids. *FEMS Microbiology Letters* **275**, 312-318 (2007).
56. L. G. Airich *et al.*, Membrane Topology Analysis of the *Escherichia coli* aromatic amino acid efflux protein YddG. *Journal of Molecular Microbiology and Biotechnology* **19**, 189-197 (2010).
57. B. E. L. Morris, R. Henneberger, H. Huber, C. Moissl-Eichinger, Microbial syntrophy: interaction for the common good. *FEMS Microbiology Reviews* **37**, 384-406 (2013).
58. O. Ponomarova, K. R. Patil, Metabolic interactions in microbial communities: untangling the Gordian knot. *Current Opinion in Microbiology* **27**, 37-44 (2015).
59. J. Swire, Selection on synthesis cost affects interprotein amino acid usage in all three domains of life. *Journal of Molecular Evolution* **64**, 558-571 (2007).
60. J. L. Barker *et al.*, Synthesizing perspectives on the evolution of cooperation within and between species. *Evolution* **71**, 814-825 (2017).
61. S. Westhoff, A. Kloosterman, S. F. A. van Hoesel, G. P. van Wezel, D. E. Rozen, Competition sensing alters antibiotic production in *Streptomyces*. *bioRxiv* 10.1101/2020.01.24.918557, 2020.2001.2024.918557 (2020).
62. J. L. Bronstein, Our Current Understanding of Mutualism. *The Quarterly Review of Biology* **69**, 31-51 (1994).
63. E. T. Kiers, R. A. Rousseau, S. A. West, R. F. Denison, Host sanctions and the legume–rhizobium mutualism. *Nature* **425**, 78-81 (2003).
64. M. McFall-Ngai, Hawaiian bobtail squid. *Current Biology* **18**, R1043-R1044 (2008).
65. H. Ogata *et al.*, KEGG: Kyoto Encyclopedia of Genes and Genomes. *Nucleic Acids Research* **27**, 29-34 (1999).

66. I. M. Keseler *et al.*, EcoCyc: a comprehensive database of *Escherichia coli* biology. *Nucleic Acids Research* **39**, D583-D590 (2010).
67. T. Baba *et al.*, Construction of *Escherichia coli* K-12 in-frame, single-gene knockout mutants: the Keio collection. *Molecular Systems Biology* **2**, 2006.0008 (2006).
68. L. C. Thomason, N. Costantino, D. L. Court, *E. coli* genome manipulation by P1 transduction. *Current Protocols in Molecular Biology* **79**, 1.17.11-11.17.18 (2007).
69. A. R. Joyce *et al.*, Experimental and computational assessment of conditionally essential genes in *Escherichia coli*. *Journal of Bacteriology* **188**, 8259-8271 (2006).
70. M. Vanstockem, K. Michiels, J. Vanderleyden, A. P. Van Gool, Transposon Mutagenesis of *Azospirillum brasilense* and *Azospirillum lipoferum*: Physical analysis of Tn5 and Tn5-Mob insertion mutants. *Applied and Environmental Microbiology* **53**, 410-415 (1987).
71. Y. Tapuhi, D. E. Schmidt, W. Lindner, B. L. Karger, Dansylation of amino acids for high-performance liquid chromatography analysis. *Analytical Biochemistry* **115**, 123-129 (1981).
72. T. Takeuchi, "1.2.5. - HPLC of amino acids as dansyl and dabsyl derivatives" in Journal of Chromatography Library, I. Molnár-Perl, Ed. (Elsevier, 2005), vol. 70, pp. 229-241.
73. S. Kumar, G. Stecher, M. Li, C. Knyaz, K. Tamura, MEGA X: Molecular Evolutionary Genetics Analysis across Computing Platforms. *Molecular Biology and Evolution* **35**, 1547-1549 (2018).
74. I. Letunic, P. Bork, Interactive Tree Of Life (iTOL): an online tool for phylogenetic tree display and annotation. *Bioinformatics* **23**, 127-128 (2006).
75. J. Zimmermann, C. Kaleta, S. Waschina, gapseq: Informed prediction of bacterial metabolic pathways and reconstruction of accurate metabolic models. *bioRxiv* 10.1101/2020.03.20.000737, 2020.2003.2020.000737 (2020).
76. P. D. Karp, M. Riley, S. M. Paley, A. Pellegrini-Toole, The metaCyc database. *Nucleic Acids Research* **30**, 59-61 (2002).
77. E. Boutet, D. Lieberherr, M. Tognolli, M. Schneider, A. Bairoch, "UniProtKB/Swiss-Prot" in plant bioinformatics: Methods and protocols, D. Edwards, Ed. (Humana Press, Totowa, NJ, 2007), 10.1007/978-1-59745-535-0_4, pp. 89-112.
78. J. Ye, S. McGinnis, T. L. Madden, BLAST: improvements for better sequence analysis. *Nucleic Acids Research* **34**, W6-W9 (2006).
79. S. Devoid *et al.*, "Automated genome annotation and metabolic model reconstruction in the SEED and Model SEED" in systems metabolic engineering: Methods and Protocols, H. S. Alper, Ed. (Humana Press, Totowa, NJ, 2013), 10.1007/978-1-62703-299-5_2, pp. 17-45.
80. H.-G. Holzhütter, The principle of flux minimization and its application to estimate stationary fluxes in metabolic networks. *European Journal of Biochemistry* **271**, 2905-2922 (2004).
81. S. Magnúsdóttir *et al.*, Generation of genome-scale metabolic reconstructions for 773 members of the human gut microbiota. *Nature Biotechnology* **35**, 81-89 (2017).
82. K. Aden *et al.*, Metabolic functions of gut microbes associate with efficacy of tumor necrosis factor antagonists in patients with inflammatory bowel diseases. *Gastroenterology* **157**, 1279-1292.e1211 (2019).
83. R. C. Team (2013) R: A language and environment for statistical computing. (Vienna, Austria).
84. Y. Benjamini, Y. Hochberg, Controlling the False Discovery Rate: a practical and powerful approach to multiple testing. *Journal of the Royal Statistical Society: Series B (Methodological)* **57**, 289-300 (1995).

866 85. Y. Benjamini, A. M. Krieger, D. Yekutieli, Adaptive linear step-up procedures that control
867 the false discovery rate. *Biometrika* **93**, 491-507 (2006).

868